RAREFACTION AND SCALE EFFECTS ON HEAT TRANSFER CHARACTERISTICS FOR ENCLOSED RECTANGULAR CAVITIES HEATED FROM BELOW

Ammar ALKHALIDI [*1], Suhil KIWAN [2], Wael AL-KOUZ [3], Aiman ALSHARE [4], Ma'en SARI[4].

[*1] Energy Engineering Department, German Jordanian University, Amman 11180, Jordan.
[2] Mechanical Engineering Department, Jordan University of Science and Technology, Irbid, 22110, Jordan.
[3] Mechatronics Engineering Department, German Jordanian University, Amman11180, Jordan.
[4] Mechanical and Maintenance Engineering Department, German Jordanian University, Amman11180, Jordan.
[*] Corresponding author; E-mail: ammar.alkhalidi@gju.edu.jo

The fluid flow and heat transfer in a buoyancy-driven microcavity heated from below are numerically investigated. In spite of the fact that micro-cavities are widely used in micro-electro-mechanical systems, now a day, more interest in the evacuated cavity on Eqn. solar collectors are very common to reduce heat loss from the system. This paper provides a useful information for engineers to estimate heat transfer in low-pressure cavities. The finite-volume technique was used to solve the governing equations along with temperature jump and slip flow boundary conditions. The simulations are carried out for various cavity aspect ratios (H/L) and different Rayleigh number for both macro and micro fluids. The effect of Knudsen number in the rarefied flow regime (microfluidic) has also been investigated. It is shown that for both cases the effect of aspect ratios on heat transfer becomes significant at high Ra numbers and when the aspect ratio is below 5. It was also found that increasing Kn reduces the heat transfer. The interaction between Nu number, Ra number, Kn number, and the aspect ratio was investigated using the design of experiments, results show that no interaction between these parameters. To help engineers to estimate heat transfer in low-pressure cavities, widely used in solar energy applications, a correlation for Convection heat transfer coefficient is introduced.

Keywords: Horizontal microcavity, slip flow, temperature jump, Knudsen number.

1. Introduction

The recent trends of moving towards increasing the share of solar energy in the energy mix have accelerated new technological developments in the field. Due to the need of the presence of transport walls to allow solar radiation to enter the space, the use of conventional insulation materials to minimize the heat loss is impossible. Furthermore, the good understanding of heat transfer and fluid flow in micro-electro-mechanical systems (MEMS) is the key point of producing high quality and low-cost MEMS.

Natural convection in cavities at atmospheric pressure or higher of various boundary conditions has been extensively studied and documented. Naffouti and Djebali [1] solved dimensionless governing equations to find heat transfer rates by Lattice Boltzmann method. This was done considering a two-dimensional natural convection flow in a square enclosure containing isothermal hot source placed asymmetrically at the bottom wall. Results were analyzed and documented [1]. Globe and Dropkin [2] presented an experimental investigation of convection heat transfer between two horizontal plates filled with liquids heated from below. The heat transfer coefficients, as confirmed by the results for all investigated liquids, may be determined from Eqn. (1).

$$Nu = 0.069 Ra^{1/2} Pr^{0.074} \tag{1}$$

Where the characteristic dimensions for the Nu and Ra numbers were the spacing between the copper plates.

Numerical investigation of rarefied gas inside microcavities of a wavy microchannel flow was done by Alshare et al. [3]. Authors used Navier Stokes Fourier equation (NSF) with temperature jump and velocity slip conditions. They found that the amplitude of the wavy channel affects the heat transfer rates. Al-Kouz et al. [4] used the same formulation in solving the steady two-dimensional, laminar, natural convective heat transfer for low-pressure gaseous flows in the annulus region between two concentric horizontal cylinders. They investigated the effects of Ra and Kn on the flow and heat transfer characteristics in the annulus region. Alkhalidi et al. [5] investigated the Buoyancy-driven heat transfer a conjugate cavity filled with rarefied gas. The simulations were carried out for different Ra number, conductivity ratios, Kn number, and cavity tilt angles. However, they did not investigate in details the role of cavity aspect ratio.

Polikarpov et al. [6] studied heat transfer through the binary gas mixture, confined between two infinite parallel plates. Two monoatomic gas mixtures: Ne–Ar and He–Ar were investigated for transient behavior in heat transfer caused by the sudden change of the plates' temperatures. Rovenskaya [7] investigated the use of nonlinear Shakhov model of the Boltzmann kinetic equation to find the rarefied gas flow caused by a temperature gradient in the direction tangential to a wall through a planar channel of finite length.

Boiling and condensation had been investigated in microcavity by Zhou [8], They numerically investigated the heat transfer characteristics of the aqueous n-butanol solution in the thin film region of the closed microcavity, based on an enhanced Young-Laplace equation that includes the contribution of disjoining pressure for self-rewetting binary fluids. Li [9] developed a microchannel configuration that enables more efficient utilization of the coolant through integrating multiple microscale nozzles connected to auxiliary channels as well as microscale reentry cavities on sidewalls of main microchannels.

Tatsios [10] used the Nonlinear Shakhov kinetic model and the Direct Simulation Monte Carlo (DSMC) model to simulate the fluid flow in a square cavity. He found that both models gave close results in the investigated ranges. Rana [11] utilized the R13 equations and the Navier–Stokes–Fourier equations to investigate moderately rarefied gas flow and heat transfer in square cavity heated from below. The aim of the investigation was to improve the understanding of the effect of slip flow on the thermal flow characteristics in early transition regime.

Bénard problem was investigated for a rarefied gas in literature. For example, the instability of a stationary stratified gas in the two-dimensional rectangular domain was studied by Sone et al. [12] using numerical methods. The longtime behavior (final state) of the Rayleigh–Bénard flow of a rarefied monatomic gas was investigated by Stefanov et al. [13]. The investigation was done for a set of the non-dimensional Knudsen and Froude numbers and results were documented. Stefanov [14] investigated Three-dimensional geometry with different aspect ratios Rayleigh–Bénard flow problem, the investigation was for a set of different Froude and Knudsen numbers at a fixed temperature ratio. Although authors [10-14] investigated rarefied flow inside cavities, they did not investigate the heat transfer associated with natural convection inside the cavity. That is, their main investigation was focused on fluid flow and the temperature distribution inside the cavity under different boundary conditions.

Two-dimensional, steady analysis of buoyancy-driven flow in uniform wall temperature microcavity is investigated in this work. At the micro level, the surface effects become more important than the volume effects. This fact may lead to an enhancement of the thermal transport. The flow is assumed laminar. Numerical methods were used to solve the continuum governing equations along with Maxwell slip [15], and temperature jump [16] boundary conditions. The effects of the aspect ratio and Knudsen number on the Nusselt number is investigated with respect to a range of Ra number.

2. Problem statement and solution methodology

The schematic diagram is shown in Fig. 1 shows the geometry of the cavity considered in this study. It consists of a top isothermal cold wall, bottom isothermal hot wall, and insulated sidewalls.

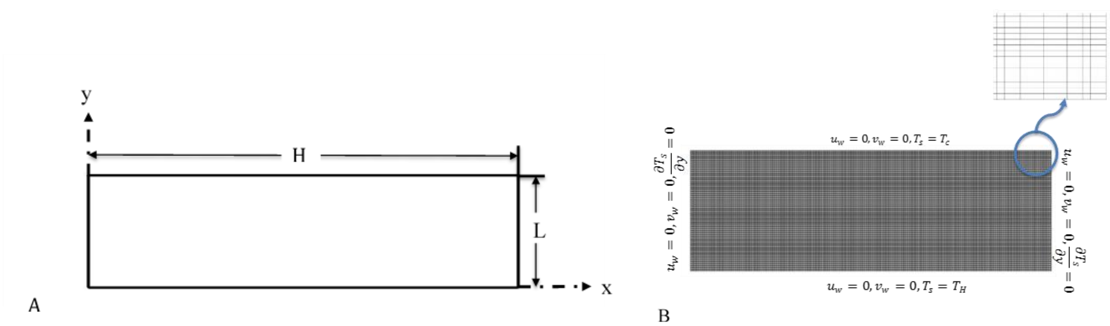

Figure 1: A) Investigation Domain and Geometry B) Mesh for and boundary conditions H/L =3 case.

The buoyancy-driven flow is assumed compressible (the density was calculated by Boussinesq approximation), steady, two-dimensional, and laminar, the thermo-physical properties are assumed to be constant. The continuum governing equations are utilized in conjunction with the slip velocity and temperature jump boundary conditions. The continuity, momentum and energy equations governing the flow and heat transfer in the cavity under consideration in Cartesian coordinates are as follows:

Continuity: $$\frac{\partial u}{\partial x}+\frac{\partial v}{\partial y}=0 \tag{2}$$

x- momentum: $$\rho\left(u\frac{\partial u}{\partial x}+v\frac{\partial u}{\partial y}\right)=-\frac{\partial P}{\partial x}+\mu\left[\frac{\partial^2 u}{\partial x^2}+\frac{\partial^2 u}{\partial y^2}\right] \tag{3}$$

y-momentum: $$\rho\left(u\frac{\partial v}{\partial x}+v\frac{\partial v}{\partial y}\right)=-\frac{\partial P}{\partial y}-\rho g+\mu\left[\frac{\partial^2 v}{\partial x^2}+\frac{\partial^2 v}{\partial y^2}\right] \tag{4}$$

Energy: $$\rho C_p\left(u\frac{\partial T}{\partial x}+v\frac{\partial T}{\partial y}\right)=k\left[\frac{\partial^2 T}{\partial x^2}+\frac{\partial^2 T}{\partial y^2}\right] \tag{5}$$

The boundary conditions for the problem are:

(a) the finite temperature at the outer surfaces of the bottom and top walls:

$$T=T_h \qquad at\ y=0 \tag{6}$$

$$T=T_c \qquad at\ y=L \tag{7}$$

(b) Colin [17] reported the Slip-condition and temperature jump at the interfaces between the solid walls and the fluid inside the cavity as follows:

The velocity slip at all walls is given as:

$$u_w-u_g=\left(\frac{2-\sigma_v}{\sigma_v}\right)\lambda\ \frac{\partial u}{\partial y} \tag{8}$$

Since the walls are stationary ($u_w=0$), therefore, Eqn. (8) becomes

$$u_g=-\left(\frac{2-\sigma_v}{\sigma_v}\right)\lambda\ \frac{\partial u}{\partial y} \tag{9}$$

The temperature jump condition is applied at all walls as:

$$T_w-T_g=\left(\frac{2-\sigma_T}{\sigma_T}\right)\frac{2\gamma}{\gamma+1}\frac{k}{\mu c_v}\lambda\frac{\partial T}{\partial y} \tag{10}$$

For the top wall, $T=T_c$, Thus, Eqn. (8) becomes

$$T_g=T_c-\left(\frac{2-\sigma_T}{\sigma_T}\right)\frac{2\gamma}{\gamma+1}\frac{k}{\mu c_v}\lambda\frac{\partial T}{\partial y} \tag{11}$$

Similarly, the temperature of the gas at the bottom wall is given by

$$T_g=T_h-\left(\frac{2-\sigma_T}{\sigma_T}\right)\frac{2\gamma}{\gamma+1}\frac{k}{\mu c_v}\lambda\frac{\partial T}{\partial y} \tag{12}$$

The mean free path length is specified as follows [18]:

$$\lambda = \frac{k_B T}{\sqrt{2}\pi d^2 P} \tag{13}$$

Where, $k_B = 1.38066 \times 10^{-23}$ JK^{-1} is the Boltzmann constant, T the temperature (K), P the pressure (Pa), and d is the molecular diameter. Knudsen number is defined as:

$$Kn = \frac{\lambda}{L} \tag{14}$$

The spacing between hot and cold walls, shown in Fig. 1, is noted by L. Fig. 1B shows the boundary conditions. Fourier's law of conduction was used to calculate the local heat flux at the bottom wall,

$$q'' = -k_f \left.\frac{\partial T}{\partial y}\right|_{y=0} \tag{15}$$

The problem solved in this paper is steady, therefore, the heat transfer was calculated by integrating the local heat flux along the bottom wall of the cavity,

$$Q = \int_A q'' dA \tag{16}$$

The average heat transfer coefficient along the bottom wall of the cavity is calculated from:

$$\bar{h} = \frac{Q}{(T_h - T_c)A} \tag{17}$$

The Nusselt number is calculated from

$$\overline{Nu} = \frac{\bar{h}L}{k_f} \tag{18}$$

3. Solution method

The governing equations, dimensional-form, along with the boundary conditions are solved in primitive variables terms. Finite Volume Method (FVM) was used to obtain the solution, by utilizing commercial, FLUENT 18, software. CAD modeler and a meshing tool were used to create the computational domain, shown in Fig.1. For H/L =1, the mesh was increased in sizes, (40 ×40), (50 × 50)… until (100 × 100) to select an optimal mesh size. Nusselt Number was used to depict the effect of mesh. The effect was found marginal after mesh (90 × 90). To ensure the convergence of the results, a (100 × 100) mesh is used and presented. This mesh size is utilized for all simulations considered in this study.

Governing equations are discretized using second-order upwind scheme. The SIMPLE algorithm was used to tackle Pressure-velocity decoupling, and the pressure discretization was performed via the PRESTO algorithm [18]. Simulations assumed totally diffuse walls, the momentum, and thermal accommodation coefficients, $\sigma_{v,}$ and σ_T, respectively, are given a value of one in all simulations. Knudsen number was varied within the slip flow regime in the range of 0.01 to 0.1. The values of the mean free path λ were calculated according to Kn number and L (see Eqn. (12)).

The solution is considered to be converged when the mass and velocity residuals are less than 10^{-3} and when the energy residual is less than 10^{-6}.

4. Model validation

Model validation was performed by reproducing experimental results found by Glope and Dropkin [2]. The current software code was able to predict the Nusselt Number given by Eqn. 1 with a maximum error of approximately 11.5% for the cases of H/L=5 and above. More deviation in results between Eqn. 1 and CFD was found for cases with H/L less than 5. This could be attributed to the fact that Eqn. 1 has conditions set by [2] that could be used only for high H/L ratios. More investigation about aspect ratio effect will be done in the current study to find the threshold for Eqn. 1. It should be noted that at Kn=0, the no-slip condition holds true, and this corresponds to the case of the microcavity. Model validation for slip and jump boundary conditions was done by the same authors and presented in [5]. It is concluded that the current simulation technique is capable of predicting the thermal performance within an acceptable accuracy.

5. Discussion of Results

To establish a benchmark case for the no-slip boundary condition of the problem under consideration, the effect of changing the aspect ratio is studied and presented. To do so, three different aspect ratios, 3, 5 and 7 are analyzed. Fig. 3 shows marginal effect of the aspect ratio on Nu for geometries with H/L=5, and 7 and about 14% difference for the case of H/L=3 compared to the case with H/L=5, and 7 at Ra=3.66×10^6. This difference diminishes below Ra=$1\text{x}10^4$.

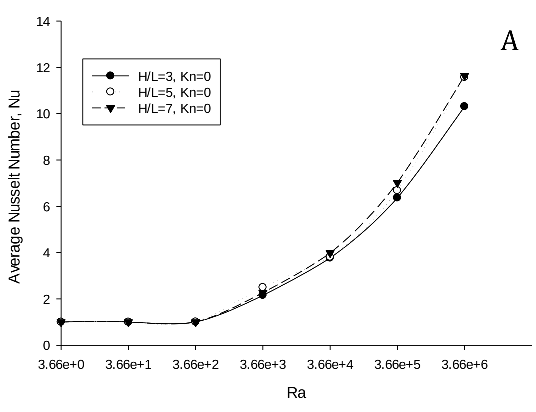

Figure 2. Aspect ratio effect on Nusselt Number for Ra Number range from 3.66 to 3.66×10^6.

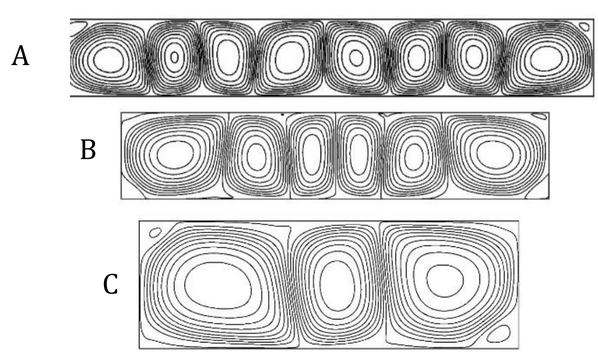

Figure 3. Velocity Stream Line for A) H/L= 7, B) H/L=5 and C) H/L=3, all for Ra= 3.66×10^6.

Furthermore, Fig. 2 shows that below Ra=3.66x10^2, conduction is the dominant mode of heat transfer for all aspect ratios, while, the convection becomes more significant at higher Ra numbers. The effect of the aspect ratio of the average Nusselt number was correlated and presented in Eqn. (19).

$$Nu = 0.186Ra^{\frac{1}{4}}\left(\frac{H}{L}\right)^{\frac{1}{5}} \tag{19}$$

Where

$$\begin{Bmatrix} Pr = 0.7 \\ 10^3 < Ra < 10^5 \\ 1 < \left(\frac{H}{L}\right) < 14 \end{Bmatrix}$$

Figure 3 shows the velocity streamlines inside cavities of different aspect ratios for the same Ra. It is clear that the number of rolling cells described by Glope and Dropkin [2] increases as the aspect ratio increases. These rolling cells characterize the advection in a horizontal fluid layer in a heated from below cavity. Results found in this work and presented in Fig. 3, show a similar pattern to that of the rolling cells flow inside the cavity described by [2].

Moreover, it was found, in this work, that number and size of rolling cells have its fingerprint on the heat transfer in the cavity; the number and, therefore, the size of rolling cells differs for different aspect ratios and it is constant for all Ra range for the same aspect ratio. At high aspect ratios, a large number of rolling cells was noticed, reducing the aspect ratio reduces the number of rolling cells inside the cavity, see Fig.3. The number, size, and strength of rolling cells control the heat transfer inside the cavity; the heat transfer increases as the number of rolling cells increases as observed for H/L=3, 5, and 7 which were discussed earlier. Secondly, for the same aspect ratios, Ra increases, the strength of the circulation of the rolling cell increases.

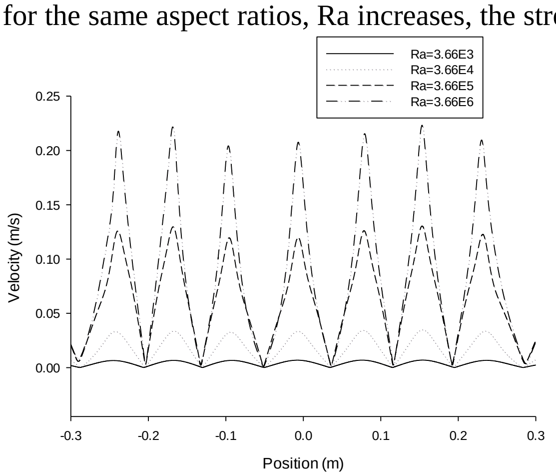

Figure 4. Velocity profile for H/L=7 at the middle of the cavity length.

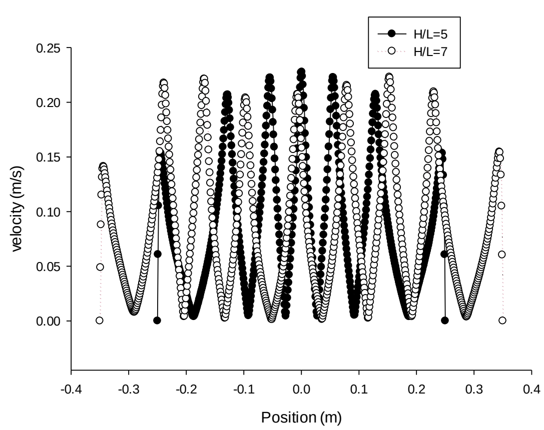

Figure 5. Velocity profile for H/L=7 and H/L=5 at the middle horizontal plane of the cavity length Ra= 3.66×10^6.

Figure 4 shows the velocity magnitude across a horizontal line located at the mid-plane of the cavity for different Ra numbers. It is clear that the increase of Ra number did not have any influence on the number of the rolling cells, however, the intensity of the velocity increases in each rolling cell. Moreover, for H/L=5, and 7, the average Nu is almost identical at Ra=3.66×10^{6}, (see Fig. 2) then it is expected to have stronger rolling cells for H/L=5 than that for H/L=7 case as noticed in Fig. 5.

5.1. Effect of Knudsen Number

Knudsen number (Kn) was used to characterize rarefied, micro and nanoscale flows. Kn measures the degree of rarefaction of the flow, it is described by the ratio of the mean free path (λ) of the characteristic length (L) of the geometry of interest. Flow regimes inside cavities are classified based on the Knudsen number into four types [19, 20]. The continuum regime, $Kn<0.01$, is in which the Navier-Stokes equations are used to describe the flow. The slip regime, $0.01<Kn<0.1$, where Navier-Stokes equations are used to describe the flow but with velocity slip and temperature jump boundary conditions. The transitional regime range $0.1<Kn<10$. Finally, the free molecular regime $10<Kn$, where the collision between particles is very rare.

The boundary slip effect on heat transfer was investigated at various Kn numbers varying from Kn=0, which represent the no-slip boundary condition, up to Kn=0.1, which cover the rarefied flow slip regime. As shown in Fig. (6), a large reduction (up to 73%) in the heat transfer is noticed due to the effect of Kn number.

To investigate the heat transfer inside the cavity at low-pressure conditions (microfluidic), results are plotted in Figs. (6-8), the heat transfer indicator was the average Nusselt number, and it was calculated based on the temperature difference between the top and the bottom surfaces of the cavity. The cavity height is used as the characteristic length.

Figure 6. Knudsen Number effect for H/L=7.

Figure 7. Temperature Profile took at the mid-height for aspect ratio H/L=7 and Ra= 3.66×10^{6}.

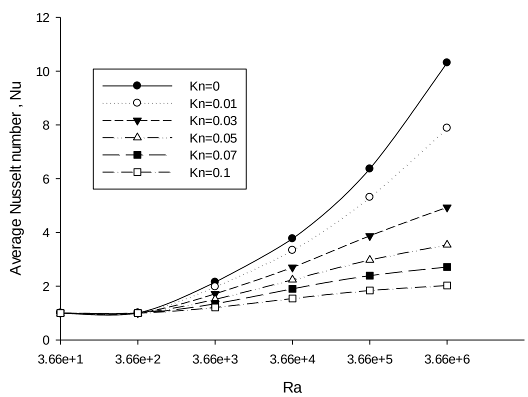

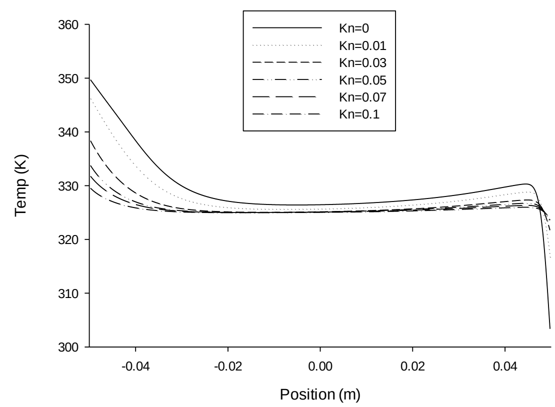

Figure 6. shows the effect of Ra number on the heat transfer for different Kn numbers. Varying Kn number between 0.01 and 0.1, a significant drop in heat transfer occurs. The rate at which Nu number decreases varies between 60 to 80% when compared to the macro fluidic case, for which Kn=0. Heat transfer reduction due to the increase in Kn could be attributed to the boundary effects (velocity slip and temperature jump). Figure 7 shows that the temperature jump at the wall results in reducing the temperature of the gas inside the cavity. This will result in reducing the driving buoyancy force (which is due to the temperature difference across the cavity) to move the fluid inside the cavity.

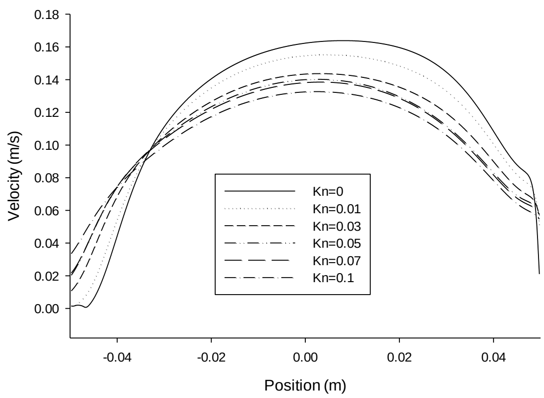

Figure 8. Velocity variation for different Kn number at mid-height for aspect ratio H/L=7 and Ra= 3.66×10⁶.

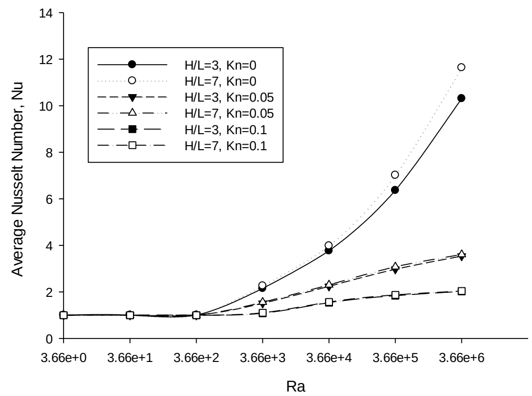

Figure 9. Geometrical effect on Nusselt Number for different H/L and Knudsen Number.

Figure 8 shows that as Kn number increases, the velocity of the air across the cavity decreases, which will reduce the advection effects, and thus the convective heat transfer is decreased. Results presented in Fig. 9 show the variation of average Nusselt number with Ra number for different aspect ratios and the whole range of Knudsen number. It is clear that the effect of changing the aspect ratio of the Nu number is negligible, as it does not exceed 2% difference, for the case of H/L=3 compared to H/L=7 case. This effect was correlated in Eqn. 20.

$$Nu = 0.0777 Ra^{0.182} Kn^{-0.404} H/L^{0.0677} \tag{20}$$

Where

$$\begin{Bmatrix} 0.01 < Kn < 0.1 \\ 10^3 < Ra < 10^5 \\ 1 < H/L < 14 \end{Bmatrix}$$

As a special case of Eqn. 20, for the aspect ratio H/L<7, the Nu number can be calculated using Eqn. 21.

$$Nu = 0.0846 Ra^{0.182} Kn^{-0.404} \tag{21}$$

Where

$$\begin{Bmatrix} 0.01 < Kn < 0.1 \\ 10^3 < Ra < 10^5 \\ H/L < 7 \end{Bmatrix}$$

Rather than using the above relation, it will be more convenient for engineers to use a simplified form for a special case of the low-pressure cavity filled with air, Eqn. (14) was utilized to estimate Kn number. Using the following data $k_B = 1.38066 \times 10^{-23}$ JK^{-1} and σ=3.71 angstroms, the convective heat transfer coefficient was correlated to the following:

$$h = 7.785 \frac{(T_H - T_C)^{0.134} P^{0.415}}{L^{0.183} T_{avg}^{0.549}} \tag{22}$$

Where

$\left\{0 < \frac{T_{avg}}{PL} < 4{,}400\right\}$, Where P is in Pascal and T is in Kelvin

6. Conclusions

The geometrical aspect ratios effect on heat transfer was investigated inside a no-slip boundary conditions cavity heated from below with insulated sidewalls. It was found that the change in the aspect ratio below H/L =5 has a high effect on the Nu number, while it has a marginal effect for ($H/L \geq 5$). It was found that flow pattern inside cavities is represented by the number, size, and the strength of stable rolling cells affects the heat transfer inside the cavity.

The microfluidic cavity has been investigated as well, and it was found that increasing Kn number in the rarefied flow regime reduces the heat transfer in the cavity for all aspect ratios due to the reduction in the velocity and temperature in the stable rolling cells. Furthermore, it was found that the effect of the aspect ratio is in general low, however, it becomes marginal by increasing Kn. Correlation of Nu number among Ra number, Kn number, and the aspect ratio is proposed. The correlation is valid for Pr number equals to 0.7 and within the investigated conditions, which reflects rarefied flow.

Nomenclature

A	- Area, [m^2]
d	- diameter of gas molecules, [m]
DSMC	- direct simulation Monte Carlo
g	- gravitational acceleration, [ms^{-2}]
h	- average heat transfer coefficient, [$Wm^{-2}\ K^{-1}$]
k_f	- thermal conductivity of air, [$Wm^{-1}K^{-1}$]
k_B	- the Boltzmann constant, [JK^{-1}]
Kn	- Knudsen number (λ/L), [-]
L	- length of cavity of the computational domain, [m]
NSF	- Naviere Stokes Fourier equation
Nu	- average Nusselt number (hL/k_f), [-]
P	- pressure, [Pa]
Pr	- Prandtl number ($v/\propto$), [-]
R	- universal gas constant
Ra	- Rayleigh number ($g\beta\Delta TL_c^3/v\alpha$), [-]
T	- temperature, [K]
T_{avg}	- average temperature ($(T_H+T_C)/2$), [K]
T_w	- cavity wall temperature, [K]
u	- velocity in x-axis, [ms^{-1}]
v	- velocity in y-axis, [ms^{-1}]

x - axial coordinate, [m]

y - vertical coordinate, [m]

Q - heat transfer rate, [W]

Greek Symbols

B - thermal expansion, [1K^{-1}]

γ - ratio of the specific heat (c_p/c_v),[-]

λ - molecular mean free path, [m]

ν - kinematic viscosity, [m^{2}s^{-1}]

ρ - density of air, given by ideal gas equation (P/RT), [kgm^{-3}]

σ - Lennard-Jones characteristic length (Ao)

σ_T - thermal accommodation coefficient

σ_v - momentum accommodation coefficient

REFERENCES

[1] Naffouti, T., Djebali, R., Natural Convection Flow and Heat Transfer in Square Enclosure Asymmetrically Heated from Below: A Lattice Boltzmann Comprehensive Study, *Computer Modeling in Engineering & Sciences, vol. 88(3),* (2012), pp. 211-228.

[2] Globe, S., Dropkin, D., Natural- Convection Heat Transfer in Liquids Confined by Two Horizontal Plates and Heated From Below, *Journal of heat transfer, Vol. 81(1)*, (1959), pp. 24-28.

[3] Alshare, A., Al-Kouz, W., Kiwan, S., Alkhalidi A., Haderd, M., Computational modeling of gaseous flow and heat transfer in a wavy microchannel, *Jordan Journal of Mechanical and Industrial Engineering, Vol. 10 (1)*, (2016), pp. 75- 83.

[4] Al- Kouz, W., Alshare, A., Alkhalidi, A., Kiwan, S., Two dimensional analysis of low pressure flows in the annulus region between two concentric cylinders, *SpringerPlus, 5:529*, (2016), DOI 10.1186/s40064-016-2140-6, 2016.

[5] Alkhalidi, A., Kiwan, S., Al-Kouz, W., Alshare, A., Conjugate heat transfer in rarefied gas in enclosed cavities. *Vacuum. Vol. 130*, (2016), PP.137-145.

[6] Polikarpov, A., Ho, M., Graur, I., Transient heat transfer in a rarefied binary gas mixture confined between parallel plates due to a sudden small change of wall temperatures. *International Journal of Heat and Mass Transfer. Vol. 101*, (2016), pp. 1292-1303.

[7] Rovenskaya, O., Numerical investigation of gas–surface scattering dynamics on the rarefied gas flow through a planar channel caused by a tangential temperature gradient. *International Journal of Heat and Mass Transfer. Vol. 89*, (2015), pp. 1024-1033.

[8] Zhou, S., Zhou, L., Du, X., Yang, Y., Heat transfer characteristics of evaporating thin liquid film in closed microcavity for self-rewetting binary fluid. *International Journal of Heat and Mass Transfer. Vol. 108*, (2017) pp.136-145.

[9] Li, W., Qu, X., Alam, T., Yang, F., Chang, W., Khan, J., Li, C., Enhanced flow boiling in microchannels through integrating multiple micro-nozzles and reentry microcavities. *Applied Physics Letters. Vol. 110(1)*, (2017), pp. 014104.

[10] Tatsios G, Vargas MH, Stefanov SK, Valougeorgis D. Nonequilibrium Gas Flow and Heat Transfer in a Heated Square Microcavity. *Heat Transfer Engineering, Vol. 37(13-14)*, (2016), pp.

1085-95.
[11] Rana AS, Mohammadzadeh A, Struchtrup H. A numerical study of the heat transfer through a rarefied gas confined in a microcavity. *Continuum Mechanics and Thermodynamics. Vol. 1;27(3)*, (2015), PP. 433-46.
[12] Sone, Y., Aoki, K. and Sugimoto, H., The Be´nard problem for a rarefied gas: Formation of steady flow patterns and stability of array of rolls, *Phys. Fluids, Vol. 9 (12)*, (1997), PP. 3898.
[13] Stefanov, S., Roussinov V. and Cercignani, C., Rayleigh–Bénard flow of a rarefied gas and its attractors. III. Three-dimensional computer simulations, *Phys. Fluids*, *Vol. 19*, (2007), PP. 124101.
[14] Stefanov, S., Roussinov, V. and Cercignani, C., Rayleigh–Be´nard flow of a rarefied gas and its attractors. I. Convection regime, *Physics of Fluids*, *Vol. 14 (7)*, (2002), PP. 2255.
[15] J.C. Maxwell, on stresses in rarefied gases arising from inequalities of temperature, *Philos. Trans. Roy. Soc. Lond. Vol. 170*, (1879), pp.231–256.
[16] M. von Smoluchowski, Ueber Wärmeleitung in verdünnten Gasen, *Ann. Phys. Chem. Vol.64*, (1898), pp. 101–130.
[17] S. Colin, *Heat Transfer and Fluid Flow in Minichannels and microchannels: Single-phase gas flow in microchannels*, Elsevier Ltd, 2006.
[18] Ansys, Fluent Documentation.
[19] Schaaf S, Chambre P., *Flow of Rarefied Gases*, Princeton Univ. Press,Princeton, 1961.
[20] Cercignani S, Lampis M, *Rarefied gas dynamics*, Academic Press, New York, 1974.

[21] Glaser, S. (Red.); Vakuum-Isolierglas (VIG), Abschlussbericht zum Verbund, *Verband Deutscher Maschinen- und Anlagenbau e. V. (VDMA)*, Frankfurt (Hrsg.), 55 S., (2007), FKZ 0327366A-G.
[22] D. Goswami and F. Kreith, *Energy Conversion*, CRC Press, Taylor & Francis Group 6000 Broken Sound Parkway NW, Suite 300, 2007.